Electronic structure of $In_{1-x}Ga_xAs/GaAs$ strained quantum wells with a δ-doped layer

1996 J. Phys.: Condens. Matter 8 1705

(http://iopscience.iop.org/0953-8984/8/11/014)

J. Phys.: Condens. Matter **8** (1996) 1705–1712. Printed in the UK

Electronic structure of $In_{1-x}Ga_xAs/GaAs$ strained quantum wells with a δ-doped layer

J H Oh†, K J Chang† and G Ihm‡

† Department of Physics, Korea Advanced Institute of Science and Technology, Taejon 305-338, Korea

‡ Department of Physics, Chungnam National University, Taejon 305-764, Korea

Received 6 November 1995

Abstract. We investigate the electronic structure of $In_{1-x}Ga_xAs/GaAs$ strained quantum wells and the effects of δ-doping on the density of states, effective mass, and transition energies via an exact treatment of the Pikus–Bir Hamiltonian. As the carrier density of the δ-doped layer increases, both the conduction and valence subbands exhibit decreasing behaviour, while the density of states and the effective masses are little affected by δ-doping. In this case, since the valence subbands decrease more rapidly with doping concentration, the energies of the transitions from the first valence subband to the conduction states are found to increase.

$In_{1-x}Ga_xAs/GaAs$ strained layer quantum wells have been receiving much attention because of the scientific interest and technological applications for devices [1–3]. Since the lattice constant of GaAs is smaller than those for $In_{1-x}Ga_xAs$ alloys, the $In_xGa_{1-x}As$ quantum well is under compressive strain, which affects the band structure of this material. The hydrostatic component of the strain increases the band gap, reducing the difference between the band gaps of the barrier and well, whereas the shear component of the strain splits off the degenerate valence bands at the Γ_8 point. As a consequence, the heavy-hole state is raised while the light-hole energy state is lowered. Such a splitting of the valence bands leads to interesting band alignments. In $In_{1-x}Ga_xAs/GaAs$ strained quantum wells, recent experiments showed that the band offset between the heavy-hole bands forms a type-I superlattice, while a type-II structure appears for the light-hole bands [2].

In this paper we investigate the energy dispersion, the density of states, and the effect of δ-doping on the electronic structure in $In_{1-x}Ga_xAs/GaAs$ strained quantum wells. We calculate the energy levels by solving the Luttinger–Kohn Hamiltonian which includes the strain effect caused by the lattice mismatch between $In_{1-x}Ga_xAs$ and GaAs [4]. We find an anisotropic feature in the valence subbands over the $\boldsymbol{k}$-space, which deviates slightly from a parabolic dispersion. The calculated density of states exhibits a staircase shape which is typical of a two-dimensional electron system. The electronic structure of a δ-doped quantum well is examined by treating self-consistently electron–electron interactions within the Hartree approximation. With the increasing of free-carrier density in the δ-doped layer, the energy separations between the conduction and valence subbands are found to increase, while the effective masses are little affected.

In our calculations, quantum wells are modelled as a multilayered heterostructure grown along the [001] direction, which consists of an $In_{1-x}Ga_xAs$ single quantum well and two adjacent GaAs layers surrounded by buffer layers which are introduced for computational convenience. Since the lattice constant of $In_{1-x}Ga_xAs$, $a(x)$, is larger than that of GaAs,

0953-8984/96/111705+08$19.50

a_0, a compressive strain on the lateral plane exists in the $In_{1-x}Ga_xAs$ well if the GaAs layer has enough thickness to maintain its own lattice constant. Then, taking into account cubic symmetry, the strain tensors are written as

$$\epsilon_{xx} = \epsilon_{yy} = \frac{a_0 - a(x)}{a_0} \qquad \epsilon_{zz} = -2\frac{C_{12}}{C_{11}}\epsilon_{xx} \qquad \epsilon_{xy} = \epsilon_{yz} = \epsilon_{zx} = 0 \tag{1}$$

where C_{11} and C_{12} are the elastic constants of $In_{1-x}Ga_xAs$.

In an effective-mass theory with the energy $E_0 = \hbar^2/m_0 l_0^2$, length l_0, and free-electron mass m_0 set to one, the conduction subbands are described by the Hamiltonian

$$H_{el} = k_z \frac{1}{2m^*(z)} k_z + \frac{k^2}{2m^*(z)} + V_e(z) + C_1(\epsilon_{xx} + \epsilon_{yy} + \epsilon_{zz}) + V_{ex}(z) \tag{2}$$

where $k^2 = k_x^2 + k_y^2$, $k_z = -\mathrm{i}\,\partial/\partial z$, $m^*(z)$ is the effective mass of an electron, C_1 is the deformation potential of the conduction band, and $V_{ex}(z)$ is an external potential such as a Hartree potential or electric field. To preserve the flux conservation of wave functions at interfaces, we employ the kinetic energy operator suggested by Ben Daniel and Duke [5]. Neglecting strain effects, the confinement potential $V_e(z)$ for electrons is represented by

$$V_e(z) = \begin{cases} E_g & \text{in the barriers} \\ E_g - \Delta E_c^0 & \text{in the well} \end{cases} \tag{3}$$

where E_g is the band gap of GaAs and ΔE_c^0 is the conduction band discontinuity between GaAs and $In_{1-x}Ga_xAs$ alloys. Here, the valence band maximum of GaAs is chosen as the reference of the energy scale.

To describe the valence subbands which are more complex than those in the conduction band because of the degeneracy, we use the Luttinger–Kohn Hamiltonian, taking into account strain effects, i.e., the Pikus–Bir Hamiltonian [4]. When the interaction with the spin-split state at the Γ_7 point is neglected, the Hamiltonian forms a 4×4 matrix:

$$H = \begin{pmatrix} P+Q & R & -S & 0 \\ R^* & P-Q & 0 & S \\ -S^* & 0 & P-Q & R \\ 0 & S^* & R^* & P+Q \end{pmatrix} \tag{4}$$

where

$$P \pm Q = -\frac{1}{2}(\gamma_1 \pm \gamma_2)k^2 - \frac{1}{2}k_z(\gamma_1 \mp \gamma_2)k_z - D_d(\epsilon_{xx} + \epsilon_{yy} + \epsilon_{zz}) \pm \frac{2}{3}D_u\left[\epsilon_{zz} - \frac{1}{2}(\epsilon_{xx} + \epsilon_{yy})\right] + V_h(z) + V_{ex}(z) \tag{5}$$

$$R = -\frac{\sqrt{3}}{2}[\gamma_2(k_x^2 - k_y^2) - 2\mathrm{i}\gamma_3 k_x k_y] - \left[\frac{D_u}{\sqrt{3}}(\epsilon_{yy} - \epsilon_{xx}) + \mathrm{i}\frac{2}{\sqrt{3}}D_u'\epsilon_{xy}\right] \tag{6}$$

and

$$S = -\mathrm{i}\frac{\sqrt{3}}{2}(k_x - \mathrm{i}k_y)(\gamma_3 k_z + k_z\gamma_3) + \frac{2}{\sqrt{3}}D_u'(\epsilon_{yz} + \mathrm{i}\epsilon_{zx}). \tag{7}$$

Here, γ_1, γ_2, and γ_3 are the position-dependent Luttinger parameters determined by fitting into the energy dispersions of bulk GaAs and $In_{1-x}Ga_xAs$. The deformation potentials of the valence band are defined as D_d for a hydrostatic stress, and D_u and D_u' for external stresses along the [001] and [111] directions, respectively [6]. The products of γ_3 and k_z are symmetrized to satisfy the hermiticity of the system [7], and such a symmetrized form

is important for calculating exact eigenvalues. In the absence of strain effects, the quantum well is described by the hole confinement potential $V_h(z)$:

$$V_h(z) = \begin{cases} 0 & \text{in the barriers} \\ \Delta E_v^0 & \text{in the well} \end{cases} \tag{8}$$

where ΔE_v^0 is the valence band discontinuity between GaAs and $In_{1-x}Ga_xAs$ alloys. Using a unitary transformation, the 4×4 Hamiltonian matrix can be reduced to two block-diagonalized 2×2 matrix forms [8]. To evaluate the eigenvalues of the resulting 2×2 Hamiltonian, we use a basis-expansion method, where eigenfunctions are expanded in terms of appropriate basis functions [9].

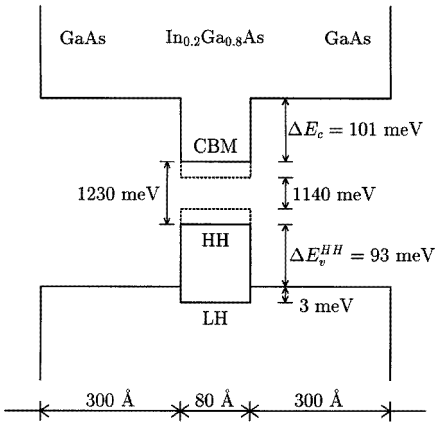

Figure 1. A schematic view of the potential profile for the $In_{0.2}Ga_{0.8}As/GaAs$ strained quantum well, where the dotted lines represent the conduction band minimum (CBM) and valence band maximum of bulk $In_{0.2}Ga_{0.8}As$. The solid lines show the type-I and type-II quantum wells for the heavy-hole (HH) and light-hole (LH) states, respectively.

The band-offset parameter Q is set to 0.52 throughout this work, which is comparable to the recently measured value [2], defined as

$$Q = \frac{\Delta E_c}{\Delta E_c + \Delta E_v^{HH}} \tag{9}$$

where ΔE_c and ΔE_v^{HH} are the conduction and valence band discontinuities, respectively, between $In_{1-x}Ga_xAs$ and GaAs, which include the energy shifts caused by strains at interfaces. This value of Q leads to a mixed type of quantum well structure where heavy holes and electrons are confined in the $In_{1-x}Ga_xAs$ layer whereas light holes are in the GaAs layer. The band profile of an $In_{0.2}Ga_{0.8}As$ strained quantum well is plotted for $Q = 0.52$ in figure 1, with the use of other physical parameters given in [10].

For a well width of 80 Å, we use 150 sine waves for a basis set to calculate the energy levels at each $\boldsymbol{k}$-point. The calculated energies are accurate with a maximum error of 10^{-3} meV. After testings, we find that the 300 Å width of the GaAs layer is enough to remove the effect of artificial buffer layers on the energy levels. Because an artificially square-shaped potential is used, the formulations for the valence subbands in equation (4) do not satisfy the flux-conservation condition at nonzero $\boldsymbol{k}$ points. However, our energy dispersions are found to be in good agreement with previous calculations which take into account the flux-conservation condition [10], as shown in figure 2. Three topmost valence subbands are heavy-hole-like, and heavy-hole states occur exactly at $\boldsymbol{k} = 0$. For nonzero $\boldsymbol{k}$-vectors, in general, the heavy-hole and light-hole states are hybridized due to the off-diagonal terms in equation (4). Although the heavy-hole and light-hole states are localized in the $In_{1-x}Ga_xAs$ and GaAs layers, respectively, their hybridization becomes significant as $\boldsymbol{k}$ increases. At a

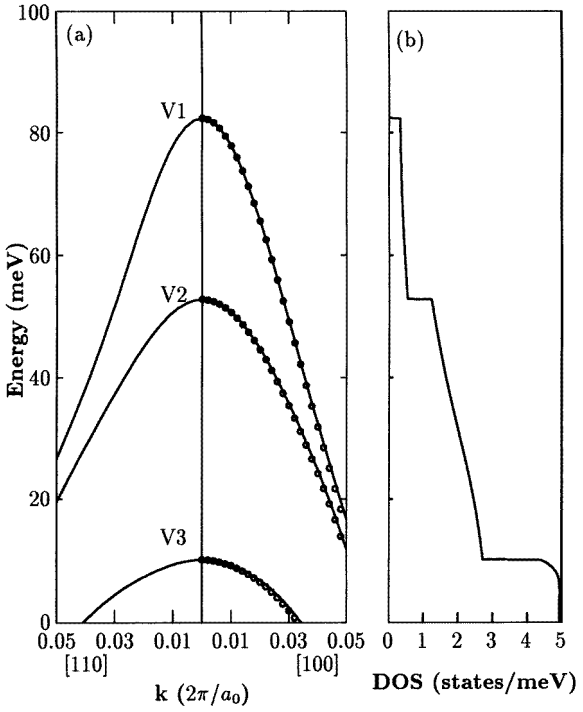

Figure 2. (a) The energy dispersions of the valence subbands (V1, V2, and V3) along the [100] and [110] directions and (b) the density of states for the $In_{0.2}Ga_{0.8}As/GaAs$ strained quantum well. Circles denote the results from the phase-matching method [10].

large-$\boldsymbol{k}$ point, for example, $\boldsymbol{k} = (0.06, 0.06)2\pi/a_0$, the hybridized states are found to have almost equal contributions from the heavy-hole and light-hole wave functions.

The calculated valence subbands along the [100] and [110] directions and the density of states are plotted in figure 2. We find that the energy dispersions are slightly anisotropic and this behaviour is caused by different values for the Luttinger parameters, $\gamma_2 = 3.34$ and $\gamma_3 = 4.14$, used for a Ga concentration of $x = 0.8$. The anisotropic feature in the energy spectrum is in fact expected because the energy dispersions of bulk $In_{1-x}Ga_xAs$ for the heavy-hole (E^-) and light-hole (E^+) states are given by

$$E^{\pm}(\boldsymbol{k}) = -\gamma_1 k^2/2 \pm \gamma_2\sqrt{k^4 - 3(1-\gamma_3^2/\gamma_2^2)k_x^2k_y^2}$$

for $k_z = 0$. Because of the anisotropic and nonparabolic energy dispersions, the density of states exhibits a feature deviating from that of a two-dimensional electron gas. In contrast to the case of $Al_{1-x}Ga_xAs/GaAs$ quantum wells, sharp peaks in the density of states are not found because an electron-like effective mass does not appear in the valence subbands [11]. The amplitudes of abrupt jumps in the density of states depend on the effective mass of each subband at $\boldsymbol{k} = 0$. In bulk $In_{0.2}Ga_{0.8}As$, the effective mass for the heavy-hole state is $m^* = 1/(\gamma_1 + 2\gamma_2) = 0.062$ along the lateral direction. However, this value in the quantum well is increased due to the confinement effect of the GaAs barriers: $m^* = 0.078$, 0.080, 0.088 for the first, second, and third topmost valence subbands, respectively.

Next we examine the electronic structure of quantum wells with a δ-doped layer. We assume that donor impurities in the δ-doped layer are fully ionized with a concentration of

N_D. For a δ-doped layer located at z_d from the centre of the well, an electron experiences both the confinement potential $V_e(z)$ (in equation (3)) and the Hartree potential $V_H(z)$, which is determined by Poisson's equation:

$$\frac{\mathrm{d}}{\mathrm{d}z}\varepsilon(z)\,\frac{\mathrm{d}}{\mathrm{d}z}V_H(z) = 4\pi e^2[N_D\,\delta(z - z_d) - n_{el}(z)] \tag{10}$$

where $\varepsilon(z)$ is the position-dependent dielectric constant. Here, the density distribution n_{el} of free carriers is given by

$$n_{el}(z) = \sum_n |\psi_{el}^n(z)|^2 N_n \tag{11}$$

where $N_n = (k_B T m^*/\pi\hbar^2)\ln[1 + \exp(E_f - E_e^n)/k_B T]$ is the occupancy of the conduction subband n with an energy E_e^n at a temperature T, E_f is the Fermi energy, and $m^* = 1/\langle\psi_n|1/m^*(z)|\psi_n\rangle$. Then, the solution of equation (10) can be written as

$$V_H(z) = 4\pi e^2 \int_{-\infty}^{z} \frac{1}{\varepsilon(s)} \int_{-\infty}^{s} [N_D\,\delta(z' - z_d) - n_{el}(z')]\,\mathrm{d}z'\,\mathrm{d}s. \tag{12}$$

Since the Hartree potential depends on the wave function, the eigenvalues are solved for self-consistently.

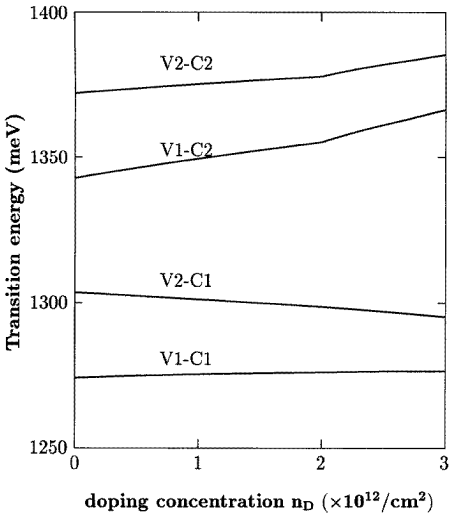

Figure 3. In the $In_{1-x}Ga_xAs/GaAs$ quantum well with a δ-doped layer at $z = 0$, various transition energies for transitions between the valence and conduction subbands plotted as functions of the doping concentration n_D.

For δ-doped quantum wells with $z_d = 0$ and various doping concentrations, we examine the electronic structure at $T = 0$ K. The energy dispersions and the densities of states are found to be similar to those for an undoped quantum well, except for a lowering of the subband energies. Since the presence of a δ-doped layer gives rise to an attractive potential, the subband energies move down for both the conduction and valence bands. Compared with the conduction subbands, since the valence band states are more localized due to large effective masses, these subband energies are decreased more rapidly by the sharp potential in the δ-doped layer. As a result of this, the transition energy between the first valence (V1) and conduction (C1) subbands is found to increase very slowly with doping concentration, as shown in figure 3. The same argument is also used for the transition between the second valence (V2) and conduction (C2) states, which exhibit more increasing behaviour. Since the wave functions of the V2 and C2 subbands have a node at $z = 0$, i.e., in the δ-doped layer, these states are less affected by δ-doping, as compared to the V1 and C1 states

which have maximum densities at $z = 0$. Thus, the V2–C1 transition energy decreases with increasing doping concentration, while the V1–C2 transition energy increases.

As the well width increases, the V1–C1 transition energy is found to decrease because of the weakening of the confinement. In the $In_{1-x}Ga_xAs$ quantum well, the compressive strain caused by the lattice mismatch enhances its band gap by

$$\Delta E_g = (1.62 + 2.30x - 2.42x^2 - 1.50x^3)/(8.33 + 3.55x).$$

However, as the Ga concentration (x) decreases, since the band gap of $In_{1-x}Ga_xAs$ decreases more rapidly, as described by the relation, $E_g^0 = 0.32 + 0.7x + 0.4x^2$ (eV), the V1–C1 transition energy decreases with decreasing x. We also note that the effective masses for various subband states exhibit decreasing behaviour as the well width increases, because electrons become more localized in the $In_{1-x}Ga_xAs$ quantum well.

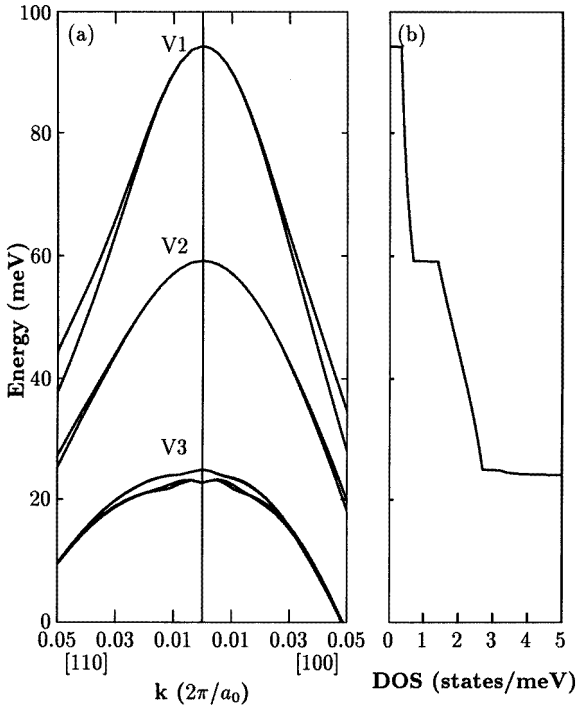

Figure 4. (a) The energy dispersions of valence subbands (V1, V2, and V3) along the [100] and [110] directions and (b) the density of states for the $In_{0.2}Ga_{0.8}As/GaAs$ quantum well with a δ-doped layer at the centre of the well and a carrier density of $n_D = 1.5 \times 10^{12}$ cm^{-2}.

If the δ-doped layer is positioned away from the centre of the well, the quantum well system loses the inversion symmetry; thus, the degenerate valence subbands at $\boldsymbol{k} \neq 0$ are split, according to equation (4). For a δ-doped layer located at $z_d = 20$ Å with $n_D = 1.5 \times 10^{12}$ cm^{-2}, the energy dispersions of the valence subbands and the density of states are plotted in figure 4. Although the position of the δ-doped layer does not significantly change the density of states, the relative positions of the energy levels are strongly affected. As the doped layer moves far from the centre of the well, the V1–C1 transition energy decreases, as shown in figure 5. In this case, electrons in the conduction band are localized in the δ-doped layer whereas holes in the valence band are outside the δ-

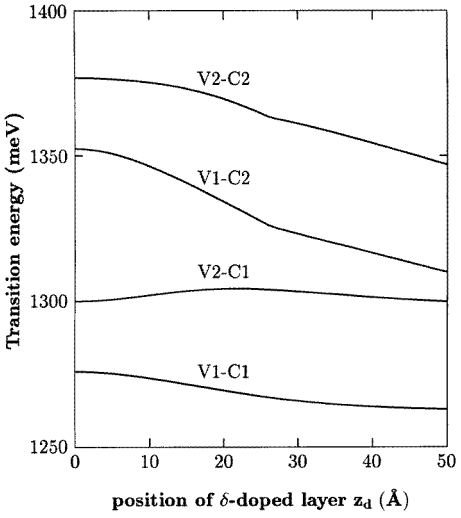

Figure 5. For the δ-doped quantum well with a carrier density of $n_D = 1.5 \times 10^{12}$ cm^{-2}, the energies of the transitions between various subband states as functions of z_d.

doped region; thus, the energy difference and the overlap of the two wave functions become smaller. This behaviour is similar to the quantum confined Stark effect that appeared in the presence of an external electric field [12]. The variations of the transition energies for transitions between various subband states with varying position of the δ-doped layer are also shown in figure 5. Other than for the transition between the C1 and V2 states, it is found that the transition energies decrease slowly with increasing z_d. For $n_D = 1.5 \times 10^{12}$ cm^{-2}, the Fermi level is found to lie between the first and second conduction bands at $z_d = 0$. As z_d increases, the Fermi level approaches to the second conduction subband, and eventually it crosses the second subband at approximately z_d = 27 Å. Then, the transition energies are strongly affected by the Fermi-level crossing, exhibiting the abruptly decreasing rate, as shown in figure 5.

In conclusion we have studied the electronic structure of $In_{1-x}Ga_xAs/GaAs$ strained quantum wells using a numerical diagonalizing scheme. Including the strain effect, the energy levels are calculated by solving the Pikus–Bir Hamiltonian exactly, and good agreements with other theoretical results are found. We find that introducing a δ-doped layer in $In_{1-x}Ga_xAs$ quantum wells increases the energy of the transition from the first valence subband to the conduction states, while the density of states and the effective mass for each subband are little affected.

Acknowledgments

This work was supported in part by the Korea Research Foundation, by the Korea Ministry of Education through grant No BSRI-94-2435, and by the CMS of Korea Advanced Institute of Science and Technology.

References

[1] Dreybrodt J, Forchel A and Reithmaier J P 1993 *Phys. Rev.* B **48** 14 741
Wang S M, Thordson J V, Andersson T G, Jiang S, Yang L X and Shen S C 1994 *Appl. Phys. Lett.* **65** 336
Piao Z S, Jeon H I, Cha S S, Lim K Y, Suh E K and Lee H J 1994 *Appl. Phys. Lett.* **65** 333
[2] Inoki C K, Ribeiro E, Lemos V and Cerdeira F 1994 *Phys. Rev.* B **49** 2246

Arnaud G, Allegre J, Lefevbre P, Matieu H, Howard L K and Dunstan D J 1992 *Phys. Rev.* B **46** 15 290
Reithmaier J P, Höger R, Riechert H, Hiergeist P and Abstreiter G 1990 *Appl. Phys. Lett.* **56** 536
[3] Menendez J, Pinczuk A, Werder D J, Sputz S K, Miller R C, Sivco D L and Cho A Y 1987 *Phys. Rev.* B **36** 8165
[4] Luttinger J M and Kohn W 1955 *Phys. Rev.* **97** 869
Pikus G E and Bir G L 1959 *Sov. Phys.–Solid State* **1** 136
[5] Ben Daniel D J and Duke C B 1966 *Phys. Rev.* **152** 683
[6] Kleiner W H and Roth L M 1959 *Phys. Rev. Lett.* **2** 334
[7] Bastard G and Brum J A 1986 *IEEE. J. Quantum. Electron.* **QE-22** 1625
[8] Boroido D A and Sham L J 1985 *Phys. Rev.* B **31** 888
[9] Ando T 1985 *J. Phys. Soc. Japan* **54** 1528
[10] Chuang S L 1991 *Phys. Rev.* B **43** 9649
[11] Altarelli M, Ekenber U and Fasolino A 1985 *Phys. Rev.* B **32** 5138
[12] Vina L, Mendez E E, Wang W I, Chang L L and Esaki L 1987 *J. Phys. C: Solid State Phys.* **20** 2803